Direct Observation of the Enthalpy Relaxation and the Recovery Processes of Maltose-Based Amorphous Formulation by Isothermal Microcalorimetry

Kohsaku Kawakami[1,2] and Yasuo Ida[1]

Purpose. The applicability of isothermal microcalorimetry (IMC) for evaluating enthalpy relaxation and recovery processes of amorphous material was assessed.

Methods. A maltose-based formulation was prepared by freeze-dry method. Differential scanning calorimetry (DSC) was used to investigate its glass transition and relaxation behaviors. IMC was applied to quantitatively analyze the relaxation and the recovery processes. The IMC data were analyzed using a derivative of the Kohlrausch-Williams-Watts equation.

Results. The glass transition temperature of the formulation and its fictive temperature stored at 15°C for 1 year were 62 and 32°C, respectively. DSC study showed that annealing below the fictive temperature increased the enthalpy recovery, but it was decreased by annealing at higher temperatures. IMC enabled direct observation of the heat flow during both the relaxation and the recovery processes. The decay constant for the recovery process (recovery time) was much smaller and less sensitive to the temperature than that for the relaxation process (relaxation time).

Conclusions. IMC was successfully used to obtain quantitative information on both relaxation and recovery processes of amorphous material. The relaxation parameters obtained by this method could explain the thermodynamic behavior of the formulation.

KEY WORDS: amorphous; differential scanning calorimetry; isothermal calorimetry; relaxation; recovery; glass transition temperature; fictive temperature; Kohlrausch-Williams-Watts equation.

INTRODUCTION

Improvement of formulation technology is becoming more and more important to develop poorly soluble compounds recently. In some cases, it may be better to give up using the crystal state and employ special dosage forms such as solid dispersions or microemulsions, although the crystal state is the most stable form physically and chemically in most cases (1–3). Despite the large number of studies in various research fields on amorphous materials, their behavior has not been fully clarified yet (4,5). Amorphous materials change their physical and thermodynamic characteristics until they reach the metastable state. This process is called relaxation (6,7), and many techniques, such as differential scanning calorimetry (DSC) (8–10), dielectric relaxation (8,11), and thermomechanical analysis (10,12), have been applied to observe the relaxation phenomena. The degree of change in the characteristics during the relaxation process can be inter-

preted by an ensemble of the exponential decay function (13). Thus, the overall decay function ϕ can be written as

$$\phi(t,T) = \sum_i g_i \exp\left(-\frac{t}{\tau_i(T)}\right) \qquad (1)$$

where g_i, T, and t are the weighting factor, temperature, and lapse of time, respectively. τ_i is a decay constant called relaxation time, which is normally around 100 s at the glass transition temperature T_g (6) and becomes significantly larger below that. Use of the heterogeneity factor β allows the equivalent equation to be obtained, as shown next:

$$\phi(t,T) = \exp\left[-\left(\frac{t}{\tau(T)}\right)^\beta\right], \quad 0 < \beta \leq 1 \qquad (2)$$

This empirically derived equation is more common because of its simplicity and is called the Kohlrausch-Williams-Watts (KWW) equation (6,7). Therefore, the excess enthalpy H_{ex} can be written as

$$H_{ex}(t,T) = H_{ex,0} \exp\left[-\left(\frac{t}{\tau(T)}\right)^\beta\right], \quad 0 < \beta \leq 1 \qquad (3)$$

where $H_{ex,0}$ is the initial excess enthalpy, that is, the excess enthalpy soon after the production of the amorphous material. Here it should be noticed that the excess enthalpy uses the metastable glass as the reference state.

Quantitative comprehension of the relaxation process is very important to control the characteristics of amorphous materials. Notably, the relaxation time τ can greatly affect both its chemical and physical stability (14). The most powerful instrument for investigating the relaxation behavior as a function of time has been the modulated-temperature DSC (16–18) because it can separate reversible from irreversible heat flow. In other words, it enables us to separately observe glass transition and relaxation enthalpy. However, what is observed in the DSC analysis is an enthalpy recovery process, and thus, it is slightly questionable to what extent it accurately reflects the enthalpy relaxation process. Isothermal microcalorimetry (IMC) has been employed to investigate various characteristics of pharmaceutical solids (19–21); however, little has been reported on its application for evaluating relaxation phenomena. Its use for obtaining the relaxation parameters has been validated recently by comparing its results with those from the conventional DSC method (22). This paper discusses the application of IMC to observe the enthalpy recovery processes, which have never been investigated by IMC, as well as the enthalpy relaxation process. The relaxation parameters obtained by the IMC method could explain various thermodynamic behaviors of the amorphous formulation.

MATERIALS AND METHODS

Materials

Maltose-based formulation was obtained from Shionogi & Co. (Osaka, Japan). The formulation consisted of 90.6 wt% of maltose, 4.7 wt% of diethanolamine, 3.9 wt% of human serum albumin, and 0.8 wt% of Tween 80. To obtain this product, 3 wt% aqueous solution was frozen at −40°C for 4 h and subjected to primary drying at −10°C for 24 h, followed

[1] Developmental Research Laboratories, Shionogi & Co., Ltd., Fukushima-ku, Osaka 553-0002, Japan.

[2] To whom correspondence should be addressed. (e-mail: kohsaku.kawakami@shionogi.co.jp)

by the secondary drying at 25°C for 4 h. The formulation was confirmed to be amorphous by the powder X-ray diffraction method. All experiments were done using the formulations stored for 1 year at 15°C after production unless otherwise mentioned. The residual water content was determined by the Karl Fisher method as 4.0 wt%.

Isothermal Microcalorimetry

A Model 2277 Thermal Activity Monitor (Thermometric AB, Sweden) was used for the IMC measurements. Two hundred milligrams of the formulation was transferred into a glass vessel in a dry box, in which the relative humidity was maintained below 5%, at room temperature (23°C). Water loss during this loading procedure could be ignored because desorption from this formulation was very slow, as shown later. Before the IMC study, sample vials were stored for 10 min in a heat oven, in which the temperature was consistent with the measurement temperature of the calorimeter. Next they were suspended at the equilibration position of the calorimeter for 20 min and immersed into the measurement position. The signal data for the first 10 min were discarded because of thermal perturbation by this immersion procedure. The same experiment was repeated three times. Figure 1 shows examples of output. As can be seen, highly reproducible signals could be obtained as a result of careful handling of the samples. Therefore, only one of the outputs at one temperature was selected for presentation hereafter. The relaxation parameters were calculated for each output by the fitting procedure shown below, and averaged values are reported with standard deviation values. Empty glass vials were used as reference.

The IMC analysis provides us direct information about the heat flow during the relaxation and the recovery processes. The generated heat flow P was fitted by the derivative of Eq. (3), that is (22):
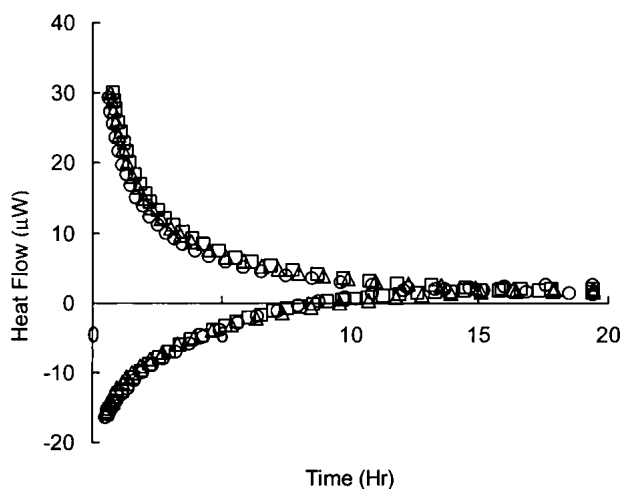

Fig. 1. Examples of outputs of the IMC experiments. These data were observed at 40°C. The endothermic curves were produced by intact formulations. The exothermic curves were for the formulation annealed at 55°C for 1 h before the measurements. Three independent measurements are differentiated by symbols (circle, triangle, and square) for both formulations. The interpretation of these curves is discussed later in the text.

$$P = H_{ex,0}\left(\frac{\beta}{\tau}\right)\left(\frac{t}{\tau}\right)^{\beta-1} \exp\left[-\left(\frac{t}{\tau}\right)^{\beta}\right] \qquad (4)$$

where

$$H_{ex,0} = \int_T^{T_g} \Delta C_p dT \qquad (5)$$

Differential Scanning Calorimetry

DSC measurements were performed on Seiko DSC 220CU (Seiko Instruments, Tokyo, Japan) with a scan rate of 5°C/min. About 3 mg of the formulation was loaded in an aluminum hermetic pan in the dry box. In annealing studies, the sample temperature was stopped at the annealing temperature T_a for 1 h in the course of the 5°C/min scan. Nitrogen was supplied as an inert gas throughout the measurement at the flow rate of 30 ml/min.

Thermogravimetric Analysis

Quasi-isothermal thermogravimetric analysis (TGA) was performed on Seiko TG/DTA 220U (Seiko Instruments, Tokyo, Japan) with a scan rate of 2°C/min. About 5 mg of the formulation was loaded in an aluminum open pan with a diameter of 5 mm and analyzed under a flow of dry air at 100 ml/min. The threshold to stop the temperature increment was 10 μg/min, and that to restart it was 5 μg/min. Isothermal TGA was measured at 30°C under the same conditions.

RESULTS

Desorption Behavior of the Formulation

Figure 2 shows the quasi-isothermal TGA analysis of the formulation. As can be seen, the water desorption was very slow below T_g (62°C, shown next). We also conducted the isothermal measurement at 30°C to find that the weight loss was only 0.3% after 5 min and 0.8% after 1 h exposure to dry air. In the following experiments, the formulation was transferred to the crimped DSC cell or the glass vial for IMC in a dry box. Because these procedures were completed within a
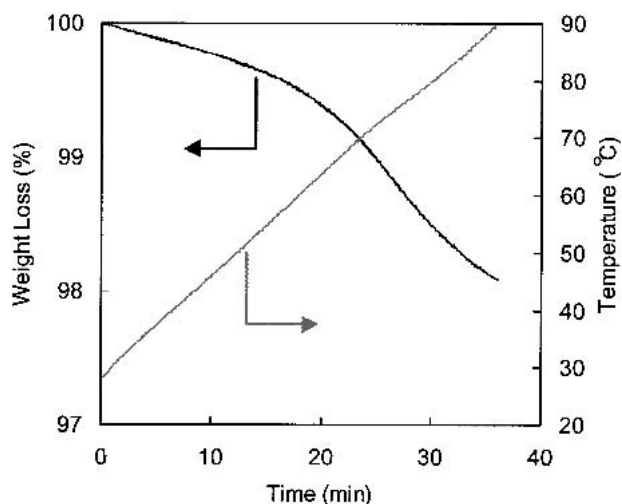

Fig. 2. Quasi-isothermal TGA curve of the intact formulation. The dark line shows the weight loss of the formulation during the heating. The gray line represents the corresponding temperature.

few minutes, the water loss during these processes could be ignored.

DSC Analysis

Figure 3 shows the DSC curves of the formulation. The intact formulation (i.e., after the storage at 15°C for 1 year; Fig. 3a) exhibited an enthalpy recovery endotherm around 60°C, followed by the glass transition at 65°C. The onset value is used for expressing T_g throughout this paper. This pattern was slightly atypical because the recovery endotherm of pharmaceutical glasses is usually observed just above the glass transition. Figure 3e shows the thermogram of the formulation, the thermal history of which was erased. This result suggested that T_g before the storage had been 62°C. ΔC_p was 0.31 J/g°C. It should be kept in mind that T_g has been known to be higher by annealing (9). Removal of water during the DSC study was not likely to be significant because, if it occurred, T_g of the thermogram (Fig. 3e) should have been much higher than Fig. 3a. Figure 3b–d shows the thermograms after annealing at various temperatures. The recovery enthalpy, which should be much smaller than the consumed excess enthalpy during the storage (see Discussion), could be estimated as 3.51 J/g from the endothermic peak area for the intact formulation. This enthalpy became slightly larger on annealing below 30°C but significantly smaller above 33°C.

Figure 4 shows the recovery enthalpy as a function of the annealing temperature. As can be seen, the enthalpy decreased with the increase of annealing temperature and completely disappeared at 52°C. This can be explained as follows.
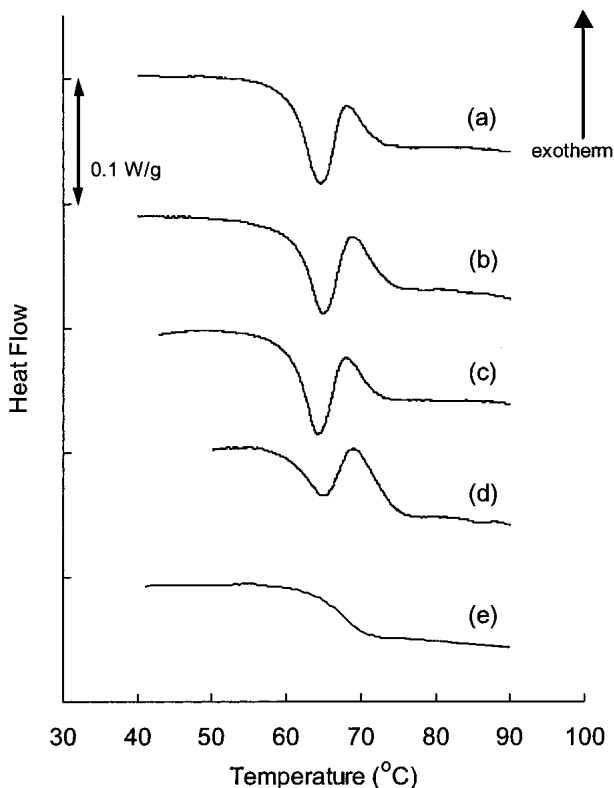

Fig. 4. Observed enthalpy recovery in the DSC analysis (open) and the calculated values using relaxation parameters from the IMC method (closed). The recovery value of the intact formulation, 3.51 J/g, was used for the calculation.

Figure 5 shows the enthalpy–temperature diagram illustrating the thermodynamic behavior of the amorphous material. Because we stored the formulation at 15°C for 1 year, the relaxation should have proceeded to some extent during the storage, as shown by arrow a. Sequential relaxation should proceed as shown by arrow b if it is annealed at a temperature below the fictive temperature T_f, which is frequently used as

Fig. 3. DSC analysis of the formulation. (a) Intact sample (i.e., stored at 15°C for 1 year). Annealed sample in the course of the temperature increment at (b) 27°C, (c) 33°C, or (d) 42°C. (e) Rescan after reaching 80°C. The cooling from 80°C to 30°C was done at 20°C/min.
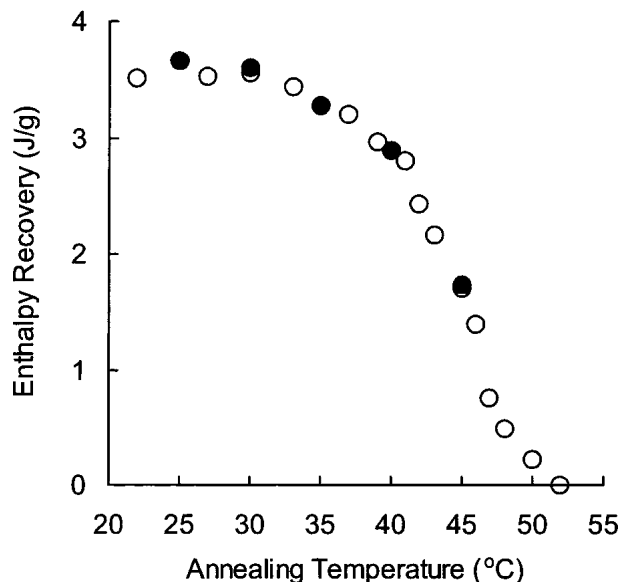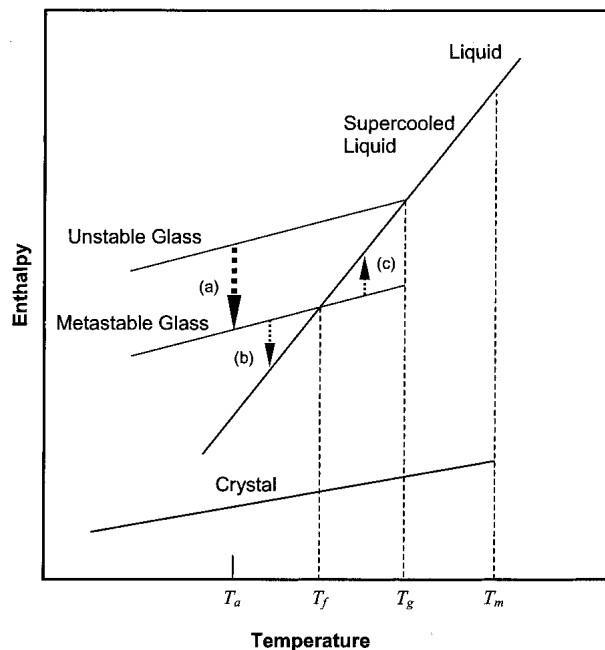

Fig. 5. An enthalpy–temperature diagram of amorphous materials. Arrow a, Relaxation process at 15°C. Arrow b, Relaxation process below 30°C. Arrow c, Recovery process above 35°C. T_a, annealing temperature; T_f, fictive temperature; T_g, glass transition temperature; T_m, melting temperature.

a measure of the structure of the amorphous material. The fictive temperature is defined by (6)

$$H(T_f) = H(T) + \int_T^{T_f} C_{pg} dT \qquad (7)$$

where $H(T)$ and C_{pg} are the enthalpy and the heat capacity of the unstable glass. T_f is the temperature at which the observed enthalpy would be the equilibrium value. If the annealing temperature is higher than T_f, the enthalpy recovery should occur as shown by arrow c. In this case, the observed endothermic peak in the DSC study should become small. Therefore, T_f of the formulation could be expected to be between 30 and 33°C.

Investigation of the Stored Formulation by IMC: Enthalpy Recovery Process

Figure 6 shows the generated heat flows from the intact formulation at various temperatures. At 25 and 30°C, very weak exothermic decay curves were observed, suggesting that no significant relaxation occurred during this measurement period. However, we observed endothermic heat flow during the first few hours, followed by exotherm, in the investigation above 35°C. At 50°C, although we observed only exothermic heat flow, it was most likely that the endothermic process had proceeded before the observation period. These observations are quite reasonable because T_f was expected to be between 30 and 33°C according to the DSC study. The isothermal observation at the temperature lower than T_f should show the exothermic enthalpy relaxation as shown by the arrow b in Fig. 5 because the formulation had not reached the metastable state yet. On the other hand, at the temperatures higher than T_f, the enthalpy recovery should be observed as the endotherm as shown by arrow c because the starting materials in the IMC measurements were below the metastable glass line. The interpretation of the exotherm after this process is given in the Discussion. These enthalpy recovery processes were analyzed by fitting the initial endothermic period using Eq. (4) for 35–45°C data. Figure 7 shows an example of this curve fitting. Although the applicability of the KWW equation to the recovery process needs further discussion, it explained the experimental results very well. The averaged best-fit parameters are shown in Table I with the standard deviation values.
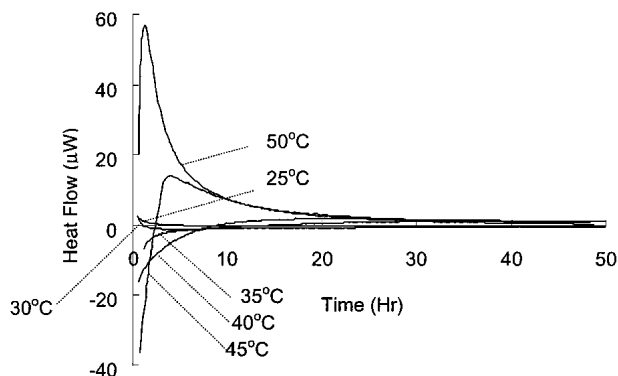

Fig. 7. An example of the fitting result of the recovery process by the KWW derivative. The raw data are expressed by open circles, and the calculated values by the solid line. This recovery was observed at 35°C after storage at 15°C. Fitting parameters are indicated in the figure.

Investigation of the Annealed Formulation by IMC: Enthalpy Relaxation Process

To observe the exothermic relaxation behavior, the formulations were stored at 55°C for 1 h and subjected to the IMC observation. This annealing was sufficient to have the material reach the metastable state because the DSC study showed that the 1-h annealing at 52°C completely erased the endothermic peak. T_f of the obtained material could be regarded as 55°C. Figure 8 shows the heat flow curves of the annealed samples measured at various temperatures. Exothermic decay curves were observed under all the temperature conditions, as expected. These curves were also fitted by Eq. (4), and the fitting example is shown as Fig. 9. The KWW derivative described the observation data very well just as in the recovery case. The averaged best-fit parameters are presented in Table I with the standard deviation values.

Estimation of Excess Enthalpy and Fictive Temperature

Figure 10 shows the Arrhenius plot for both the relaxation and the recovery processes. Although the relaxation

Fig. 6. The heat flow as a function of time for the intact formulation (i.e., after 1-year storage at 15°C). The measurement temperature is indicated in the figure.
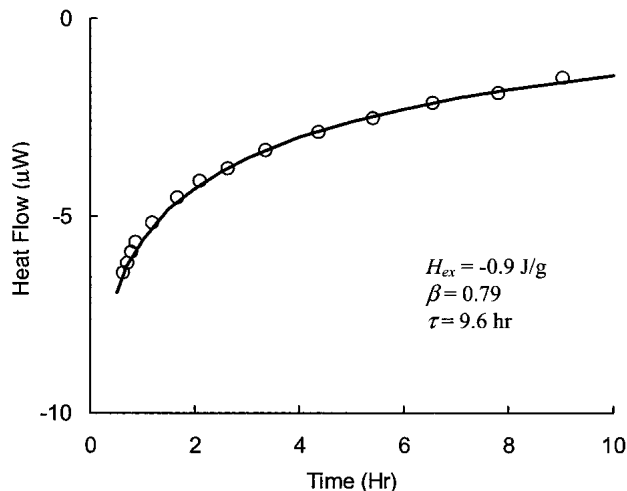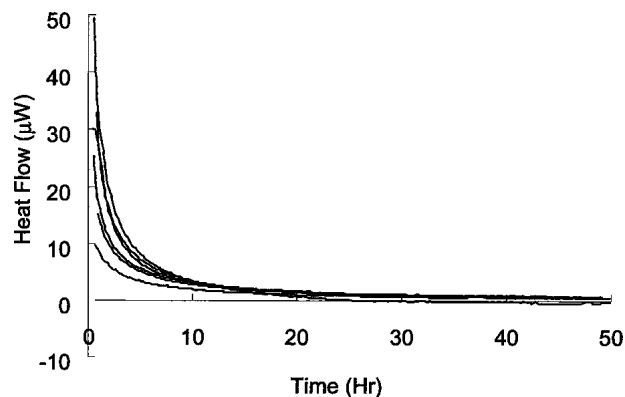

Fig. 8. The heat flow as a function of time for the annealed formulation at 55°C. The measurement temperatures were 50, 45, 40, 35, 30, and 25, respectively (top to bottom).
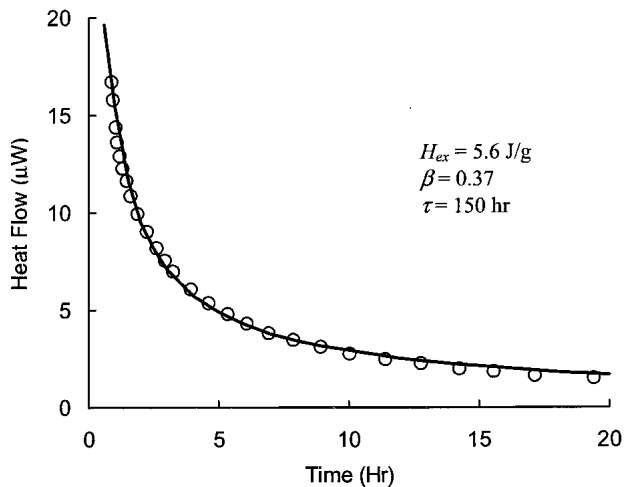
Fig. 9. An example of the fitting result of the relaxation process by the KWW derivative. The raw data are expressed by the open circles, and the calculated values are shown by the solid line. This relaxation was observed at 35°C after the 55°C annealing. Fitting parameters are indicated in the figure.

time obtained and the widely accepted relaxation time at T_g, 100 s, fell into nearly a straight line, non-Arrhenius bending was observed for the recovery process. This bending is not surprising because sugar forms fragile glass, which is known to show non-Arrhenius behavior (5,15,23), as shown by the insert of Figure 10. The activation energies were calculated as 230 kJ/mole for the relaxation and 110–220 kJ/mole for the recovery, meaning that the recovery time is less sensitive to the temperature than the relaxation time. The heterogeneity parameter β decreased with a decrease in temperature, suggesting that the heterogeneity has a greater impact on the relaxation behavior at the lower temperature. Also found was that β values for the recovery were much higher than those for the relaxation. It seems acceptable because τ for the recovery was much shorter. The absolute values of best-fit $H_{ex,0}$ were compared with the calculated ones from $\Delta C_p (T_f - T)$ in Fig. 11 by using the T_f value of 55°C for the relaxation and assuming 32°C for the recovery as fitting parameters. Although the excess enthalpies near T_f were slightly larger than the calculated values, the agreement seemed satisfactory. Therefore, T_f of the intact formulation could be determined as 32°C.

DISCUSSION

The relaxation process is driven by the energy difference between the actual state and the metastable state. Because

the energy level of the actual material is usually higher than that of the metastable state, it relaxes toward that state gradually. In this case, the exothermic heat flow should be observed. If the material is heated suddenly, its enthalpy level can be lower than that of the metastable state. This material must recover its enthalpy, and thus an endothermic heat flow is produced. IMC was a very powerful instrument to observe this rapid endothermic recovery as well as the slow exothermic relaxation. Both the relaxation and the recovery were analyzed by the KWW derivative [Eq. (4)], although its applicability to the recovery process still needs discussion. As a matter of fact, the recovery process was suggested to be an "autocatalytic" type (24), and thus a different model may be needed for the recovery process. This process was followed by the exothermic heat flow. Therefore, an energetically higher state than the metastable state seems to have been attained after the rapid recovery process. This may be explained by the difference in the translational and rotational diffusion constants near T_g, which is known as the reason for the heterogeneous domain formation (25,26). In other words, the rapid recovery might lead to a heterogeneous structure. Further investigation of this matter by IMC is likely to be very meaningful for a deeper understanding of the recovery process.

One great advantage of the IMC analysis is that it provides direct information on the heat flow during the relaxation process, as mentioned earlier. However, unlike the DSC method, it is difficult to control the thermal history precisely because erasure of the thermal history and the annealing must be done outside the instrument. Unless the relaxation before the measurement can be neglected, the relaxation cannot be analyzed precisely. If β can be approximated as 1, this problem can be overcome easily thanks to the self-similar characteristics of the exponential function. The KWW equation can be rewritten using the lapsed time t as

$$\phi(t,T) = \exp\left[-\left(\frac{t+t_1}{\tau(T)}\right)\right] \tag{8}$$

and can be transformed as

$$\phi = a \exp\left[-\left(\frac{t}{\tau(T)}\right)\right] \tag{9}$$

where

$$a = \exp\left[-\left(\frac{t_1}{\tau(T)}\right)\right] \tag{10}$$

Therefore, the relaxation time, can be obtained by simply regarding the excess enthalpy as a fitting parameter, which should be lower than the prediction from Eq. (6). In addition,

Table I. Fitting Parameters for KWW Derivative

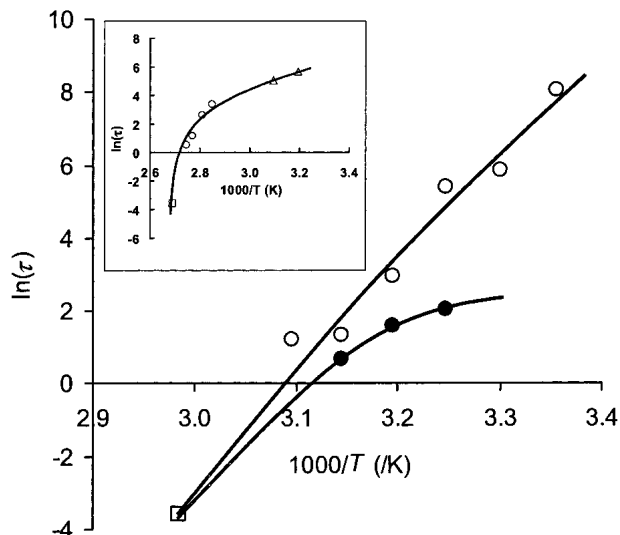| Temperature (°C)	Recovery after 15°C storage			Relaxation after 55°C annealing		
	$H_{ex,0}$ (J/g)	β	τ (h)	$H_{ex,0}$ (J/g)	β	τ (h)
50	—	—	—	3.1 ± 0.8	0.57 ± 0.24	3.4 ± 0.4
45	−3.6 ± 0.7	0.78 ± 0.10	2.0 ± 1.0	4.0 ± 1.0	0.42 ± 0.13	3.9 ± 1.6
40	−1.4 ± 0.1	0.77 ± 0.06	5.0 ± 1.0	4.9 ± 0.2	0.37 ± 0.06	19 ± 1
35	−0.9 ± 0.1	0.60 ± 0.20	7.7 ± 3.6	5.7 ± 0.4	0.28 ± 0.07	218 ± 96
30	—	—	—	7.8 ± 1.1	0.31 ± 0.01	343 ± 12
25	—	—	—	8.2 ± 1.0	0.33 ± 0.03	3133 ± 231

Fig. 10. Arrhenius plots for the relaxation time (open circles) and the recovery time (closed circles). The universal relaxation time at T_g (100 s) is also shown as a square. The error bars are omitted, but the standard deviations are indicated in Table I. Inserted graph shows the relaxation time of maltose glass obtained by K. Kawakami and M. J. Pikal (unpublished results) using temperature-modulated DSC (circles) and IMC (triangles). The universal relaxation time at T_g is also shown as a square.

this fitting procedure also provides the lapsed time, that is, the degree of relaxation before the IMC measurement. However, the relaxation time usually has a distribution; that is, β is usually lower than 1. As a matter of fact, the β value of our formulation was quite low, maybe because of the many additives. Unless β can be regarded as 1, the derivative is a little complicated.

$$P = H\left(\frac{\beta}{\tau}\right)\left(\frac{t+t_1}{\tau}\right)^{\beta-1}\exp\left[-\left(\frac{t+t_1}{\tau}\right)^{\beta}\right] \quad (11)$$

This equation has a practical problem because of four independent fitting parameters, which make the precise evaluation of each parameter difficult. Therefore, careful control of the thermal history before the measurement is favorable, notably when a low β value is expected. And the excess enthalpy value obtained by the DSC method should be employed.

The Arrhenius plot showed that the relationship between $\ln\tau$ and $1/T$ of the relaxation process was relatively linear, but this is not the case when only sugars are employed as a component. Therefore, the additives seem to have a great impact on the molecular mobility of the formulation. Among the additives, protein is known to form a relatively strong amorphous structure (27), which makes the Arrhenius plot linear. Consequently, human serum albumin may exert a great influence on molecular mobility of other components. According to the Arrhenius plot, the relaxation time at 15°C can be estimated as around 60,000 h. By supposing β as 0.3, ϕ after 1-year storage was calculated as 0.57. Thus, T_f of the stored formulation was approximately evaluated as 42°C by simple intrapolation. The experimentally obtained value 32°C is likely to be a little low. However, we did not take into account the thermal history before storage at 15°C and the temperature dependence of the heat capacity, both of which contrib-
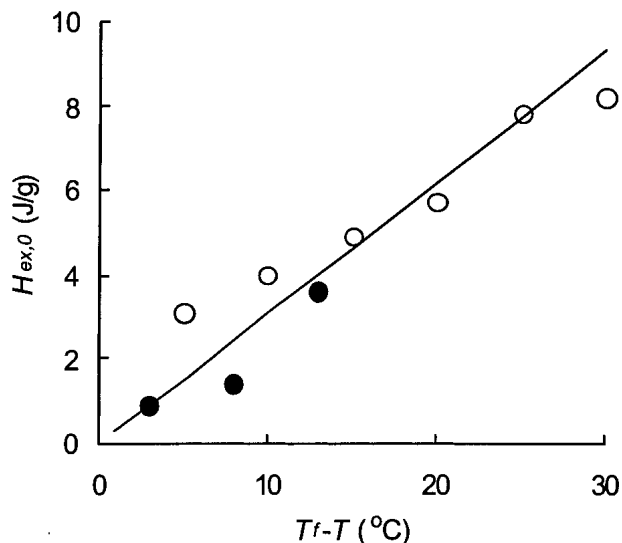

Fig. 11. Excess enthalpies obtained from the fitting procedure as a function of $T_f - T$ for the relaxation (open) and recovery (closed) processes. The line in the figure was drawn using Eq. (6), replacing T_g with T_f. The error bars are omitted, but the standard deviations are indicated in Table I.

ute to the decrease of T_f. Therefore, this discrepancy in T_f seems to be acceptable. In a similar way, the recovery time at 55°C can be calculated as 0.15 h. This gives $\phi = 0.01$ after the 1-h annealing by supposing β to be 0.8, showing that the annealing procedure was sufficient to bring the amorphous formulation to the metastable state.

As mentioned earlier, the recovery enthalpy of our formulation obtained in the DSC study should be much smaller than the relaxation enthalpy as shown by Fig. 12. Let us suppose the formulation reached state B from A during the annealing. In the DSC measurement, a typical sample follows the route B–C, and it recovers its enthalpy near T_g as shown
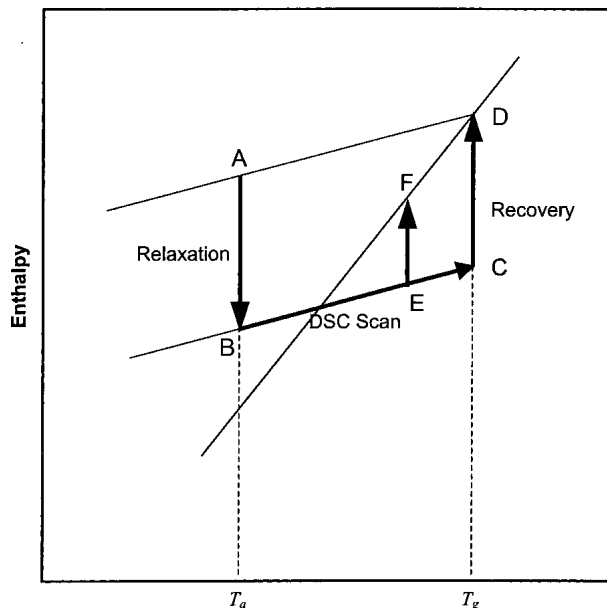

Fig. 12. An enthalpy–temperature diagram illustrating the case in which the observed recovery enthalpy is smaller than the relaxation enthalpy.

by the arrow C–D. Because there is a parallelogram A–B–C–D, the recovery enthalpy C–D is consistent with the relaxation enthalpy A–B. However, our formulation recovered its enthalpy at a much lower temperature than T_g meaning that the route for the recovery process was E–F. Therefore, the observed recovery enthalpy in the DSC measurement was much smaller than its relaxation enthalpy lost during the storage. Nevertheless, it is possible to estimate the impact of the annealing during the DSC measurement on the recovery enthalpy using the relaxation parameters obtained from the IMC measurements. We calculated the enthalpy loss (below 30°C) or gain (above 35°C) during the annealing using the parameters in Table I. The obtained recovery enthalpy values are shown in Fig. 4, which was in excellent agreement with the experimental values. This result also supports the validity of the relaxation parameters obtained by IMC. Although modulated-temperature DSC enabled more precise evaluation of the relaxation enthalpy compared to conventional DSC, it also has some specific problems such as the frequency effect (11,28–30). The application of IMC for the enthalpy relaxation study should be very helpful for understanding the relaxation and recovery mechanisms.

CONCLUSIONS

The enthalpy relaxation and the recovery processes of the maltose-based formulation were discussed with a focus on the applicability of IMC. DSC study showed that annealing below T_f, which was determined as 32°C, increased the enthalpy recovery, but it was decreased by annealing at higher temperatures. The formulation after 1-year storage at 15°C ($T_g - 50$°C) produced endothermic heat flow above T_f followed by the exotherm. The endothermic process was elucidated as the enthalpy recovery and analyzed by the KWW derivative. The relaxation process was observed by the formulation annealed near T_g, and the observed heat flow curves were also analyzed by the KWW derivative to obtain the relaxation parameters. The recovery time was much smaller and less sensitive to the temperature than the relaxation time.

REFERENCES

1. M. J. Pikal, A. L. Lukes, J. E. Lang, and K. Gaines. Quantitative crystallinity determinations for β-lactam antibiotics by solution calorimetry: Correlations with stability. *J. Pharm. Sci.* **67**:767–773 (1978).
2. T. Oguchi, E. Yonemochi, K. Yamamoto, and E. Nakai. Freeze-drying of drug-additive binary systems. II. Relationship between decarboxylation behavior and molecular states of *p*-aminosalicylic acid. *Chem. Pharm. Bull.* **37**:3088–3091 (1989).
3. Y. Guo, S. R. Byrn, and G. Zografi. Physical characteristics and chemical degradation of amorphous quinapril hydrochloride. *J. Pharm. Sci.* **89**:128–143 (2000).
4. A. P. Sokolov. Why the glass transition is still interesting. *Science* **273**:1675–1676 (1996).
5. L. Yu. Amorphous pharmaceutical solids: preparation, characterization and stabilization. *Adv. Drug Delivery Rev.* **48**:27–42 (2001).
6. I. M. Hodge. Enthalpy relaxation and recovery in amorphous materials. *J. Non-Cryst. Solids* **169**:211–266 (1994).
7. C. A. Angell, K. L. Ngai, G. B. McKenna, P. F. McMillan, and S. W. Martin. Relaxation in glass-forming liquids and amorphous solids. *Appl. Phys. Rev.* **88**:3113–3157 (2000).
8. H. Sasabe and C. T. Moynihan. Structural relaxation in poly(vinyl acetate). *J. Polym. Sci. Polym. Phys. Ed.* **16**:1447–1457 (1978).
9. E. Fukuoka, M. Makita, and S. Yamamura. Some physicochemical properties of glassy indomethacin. *Chem. Pharm. Bull.* **34**: 4314–4321 (1986).
10. B. C. Hancock, S. L. Shamblin, and G. Zografi. Molecular mobility of amorphous pharmaceutical solids below their glass transition temperatures. *Pharm. Res.* **12**:799–806 (1995).
11. V. Andronis and G. Zografi. The molecular mobility of supercooled amorphous indomethacin as a function of temperature and relative humidity. *Pharm. Res.* **15**:835–842 (1998).
12. M. Koide, R. Sato, T. Momatsu, and K. Matusita. Viscosity of lead silicate glasses below glass transition temperature by the fibre bending method. *Phys. Chem. Glasses* **36**:172–175 (1995).
13. R. Richert. Homogeneous dispersion of dielectric responses in a simple glass. *J. Non-Cryst. Solids* **172–174**:209–213 (1994).
14. D. Zhou, G. G. Z. Zhang, D. Law, D. J. W. Grant, and E. A. Schmitt. Physical stability of amorphous pharmaceuticals: Importance of configurational thermodynamic quantities and molecular mobility. *J. Pharm. Sci.* **91**:1863–1872 (2002).
15. C. A. Angell. Relaxation in liquids, polymers and plastic crystals—strong/fragile patterns and problems. *J. Non-Cryst. Solids* **131–133**:13–31 (1991).
16. V. L. Hill, D. Q. M. Craig, and L. C. Feely. Characterization of spray-dried lactose using modulated differential scanning calorimetry. *Int. J. Pharm.* **161**:95–107 (1998).
17. J. M. Hutchinson and S. Montserrat. The application of temperature-modulated DSC to the glass transition region II. Effect of a distribution of relaxation times. *Thermochim. Acta* **377**:63–84 (2001).
18. S. L. Simon. Temperature-modulated differential scanning calorimetry: theory and application. *Thermochim. Acta* **374**:55–71 (2001).
19. R. J. Willson, A. E. Beezer, J. C. Mitchell, and W. Loh. Determination of thermodynamic and kinetic parameters from isothermal heat conduction microcalorimetry: Applications to long-term reaction studies. *J. Phys. Chem.* **99**:7108–7113 (1995).
20. M. A. Phipps and L. A. Mackin. Application of isothermal microcalorimetry in solid state drug development. *Pharm. Sci. Technol. Today* **3**:9–17 (2000).
21. K. Kawakami, T. Numa, and Y. Ida. Assessment of amorphous content by microcalorimetry. *J. Pharm. Sci.* **91**:417–423 (2002).
22. J. Liu, D. R. Rigsbee, C. Stotz, and M. J. Pikal. Dynamics of pharmaceutical amorphous solids: The study of enthalpy relaxation by isothermal microcalorimetry. *J. Pharm. Sci.* **91**:1853–1862 (2002).
23. C. A. Angell. Formation of glasses from liquids and biopolymers. *Science* **267**:1924–1935 (1995).
24. G. B. McKenna. Dynamics and mechanics below the glass transition: The non-equilibrium state. *Comp. Mater. Sci.* **4**: 349–360 (1995).
25. H. Sillescu. Heterogeneity at the glass transition: A review. *J. Non-Cryst. Solids* **243**:81–108 (1999).
26. C. Y. Wang and M. D. Ediger. Anomalous translational diffusion: A new constraint for models of molecular motion near the glass transition temperature. *J. Phys. Chem. B* **104**:1724–1728 (2000).
27. J. L. Green, J. Fan, and C. A. Angell. The protein–glass analogy: Some insights from homopeptide comparisons. *J. Phys. Chem.* **98**:13780–13790 (1994).
28. S. Weyer, A. Hensel, and C. Schick. Phase angle correction for TMDSC in the glass-transition region. *Thermochim. Acta* **304/305**:267–275 (1997).
29. Z. Jiang, C. T. Imrie, and J. M. Hutchinson. Temperature modulated differential scanning calorimetry. Part I: Effects of heat transfer on the phase angle in dynamic ADSC in the glass transition region. *Thermochim. Acta* **315**:1–9 (1998).
30. D. Q. M. Craig, M. Barsnes, P. G. Royall, and V. L. Kett. An evaluation of the use of modulated temperature DSC as a means of assessing the relaxation behavior of amorphous lactose. *Pharm. Res.* **17**:696–700 (2000).